DESIGN OF THE SECOND-GENERATION ILC MARX MODULATOR*

M.A. Kemp#, A. Benwell, C. Burkhart, R. Larsen, D. MacNair, M. Nguyen, J. Olsen,
SLAC National Accelerator Laboratory, Menlo Park, CA 94025, U.S.A.

Abstract

SLAC National Accelerator Laboratory (SLAC) has initiated a program to design and build a Marx-topology modulator to produce a relatively compact, low-cost, high availability klystron modulator for the International Linear Collider (ILC). Building upon the success of the P1 Marx, the SLAC P2 Marx is a second-generation modulator whose design further emphasizes the qualities of modularity and high-availability. This paper outlines highlights of this design and presents single-cell performance data obtained during the proof-of-concept phase of the project.

INTRODUCTION

The linac klystron modulator specifications for the ILC are summarized in Table 1. Presently undergoing life testing, the SLAC P1 Marx achieves these specifications [1]. The P2 Marx design will operate to the same specifications with several fundamental differences [2, 3]. First, the Marx cell voltages are designed around the operating voltage of a single semiconductor device rather than an array of switches. This simplifies control and protection schemes. Second, output pulse regulation is achieved through regulation at the cell level. Each cell produces a flat-top pulse rather than inherent capacitor droop being compensated by a separate, external, single-point-failure device. Third, modulator construction will utilize single-side maintenance access to reduce the footprint. Forth, a hierarchical control architecture is utilized for control of the cells. This includes advanced diagnostic access as well as prognostic capabilities to determine modulator health [4, 5].

To date, extensive tests have been conducted on single cells and arrays of up to three cells. Most of the controls system hardware has been prototyped and integrated with the cells. Two versions of the P2 Marx cell have been fabricated. Data presented in this manuscript are exclusively from the first version of the cell.

Table 1: ILC klystron modulator specifications.

Peak Voltage	120 kV
Peak Current	140 A
Pulse Width	1.565 ms
Pulse Repetition Frequency	5 Hz
Pulse Flat-Top	+/- 0.5%
Average Power	137 kW
Energy Deposited in Klystron from Gun Spark	<20 J

*Work supported by the US Department of Energy under contract DE-AC02-76SF00515.
#mkemp@slac.stanford.edu

SYSTEM DESCRIPTION

Simplified cell schematic

A simplified schematic of the current version of the cell is shown in Fig. 1. Similar to the P1 Marx, the “fire” IGBT Q1 closes at the beginning of the pulse, discharging the main storage capacitor C1. The output voltage at the onset of the pulse is approximately the charge voltage of C1. Node *C* in Fig. 1 is initially at cell-low potential. As the voltage across C1 droops, the correction fire IGBT, Q3, chops at the PWM frequency, discharging C2. As a result, the voltage at node *C* ramps up. This ramp-up compensates the ramp-down on capacitor C1, resulting in a square output pulse. This regulation scheme has been termed “nested droop correction” [2].

After the pulse, node *C* must return to cell-low potential prior to the start of the next pulse. Therefore, Q4 chops and recovers the energy stored in the PWM filter capacitors back to C2. After, Q4 and Q2 close to enable recharging of the storage capacitors. Additional detail on the basic Marx charge and discharge functions is found in [1].

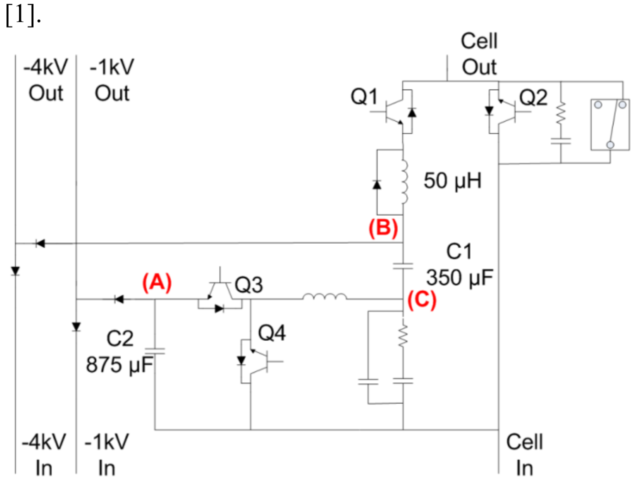

Figure 1: Simplified Marx cell schematic.

The modulator will utilize thirty-two cells to construct the output pulse. Each cell can operate at up to 4kV. Hence, up to two cells can be disabled and the modulator still provides the required output. Therefore, N+2 redundancy is achievable.

Control system

The control system for the P2 Marx is composed of three distinct platforms: application manager, hardware manager, and gate drive [4]. Figure 2 illustrates a simplified control system diagram. At the lowest level, the gate drives control and protect the IGBTs. Additionally, diagnostic and prognostic functions are

Work supported in part by US Department of Energy contract DE-AC02-76SF00515.

implemented using a microprocessor-based control card [6]. In addition, each cell has a single hardware manager. Primary tasks include distributing fire signals to the gate drives, providing second-level fault protection, monitoring of diagnostics, and implementation of the cell regulation algorithm.

A single application manager controls the modulator. This platform communicates via gigabit fibre-optic Ethernet to each of the individual cells. Presently, this is simply implemented by a PC connected to an Ethernet switch. This platform will handle tasks such as diagnostic waveform viewing and archiving, prognostic evaluation, modulator state control, modulator reconfiguration, and power supply control.

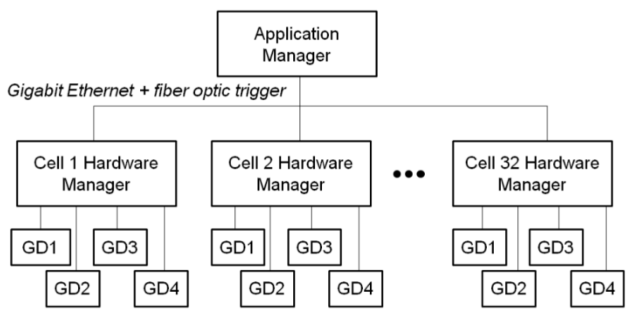

Figure 2: P2 Marx controls system diagram.

Mechanical layout

There have been two versions of the P2 Marx cell constructed at the time of this publication. The first version has been extensively characterized in single-cell operation. The second version of the cell was fabricated with an aspect ratio which allows for a more densely-packed overall modulator, incorporates higher energy density capacitors [7], and has a maintenance-friendly layout. The version 2 cell is shown in Figure 3. The power semiconductors and snubbers are to the right side of the cell. Storage capacitors and inductors are to the left. Approximate cell dimensions are 14”x26”x8” (WxLxH).

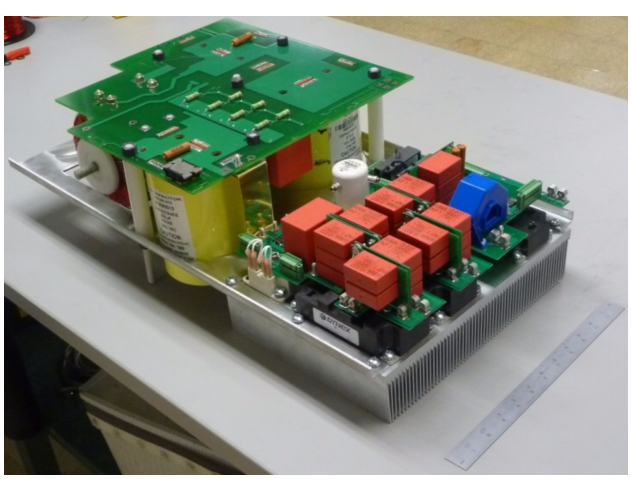

Figure 3: Photograph of second version of the P2 Marx cell prototype. Control hardware is omitted for clarity. Cell is not pictured in final form. A foot-long (~30.5 cm) ruler is included at right for scale.

A sketch of the overall modulator is shown in Figure 4. Doors along one side of the enclosure, not shown provide service access. Cells reside in individual metal cases which both shield the cell from noise as well as provide field-shaping to reduce potentially damaging corona production. The modulator is air cooled and waste heat is removed via an air-water heat exchanger.

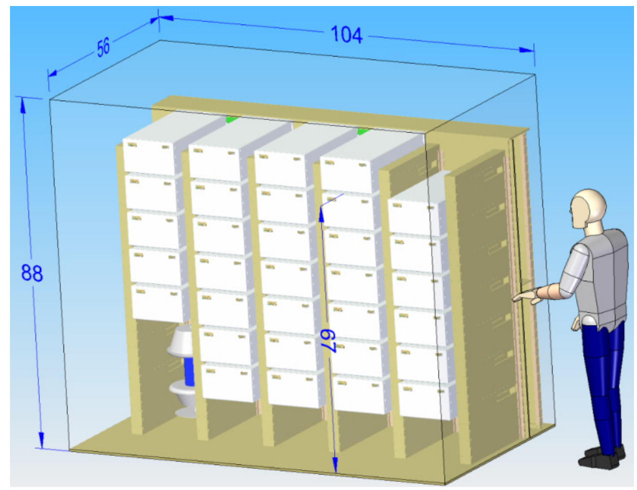

Figure 4: Preliminary sketch of the overall modulator layout. Dimensions are in inches.

Regulation Scheme

Differing from the P1 Marx, the P2 Marx will utilize a closed-loop regulation scheme. There are many potential regulation scheme implementations and strategies. Initially, a feed-forward algorithm was selected. With this scheme, each individual cell records its output voltage during the pulse. This waveform is sent to the application manager level, compared to an ideal waveform, and an error function is calculated. Using de-convolution, a new set of PWM switch timings are generated. These are transmitted back to the cell for use on the following pulse. This algorithm converges to a very accurate correction when used with a stable impedance load, such as a klystron. Operational experience with the P1 Marx and a Toshiba L-band multi-beam klystron indicate pulse-to-pulse differences in perveance are <0.1% [8].

PROOF-OF-CONCEPT EXPERIMENTAL RESULTS

Bench-top testing of a single Marx cell was completed to demonstrate the regulation scheme, test the power electronics at full peak and average power, and verify the fault tolerance of the cell. Figure 5 illustrates key measured waveforms. Shown in the top plot, both the output current and voltage remain flat over the width of the output pulse. The lower plot contains the PWM inductor current waveform as well as the voltage across Q3. As shown, up to 200A flows through the inductor during the pulse. After the pulse, the current reverses polarity during the energy recovery portion of the pulse.

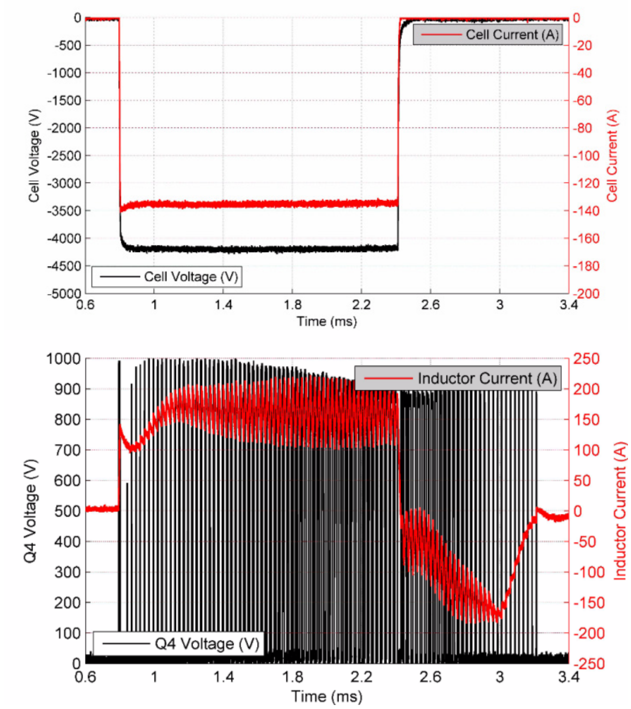

Figure 5: Measured waveforms of a single cell.

A load-arc condition was simulated with a single cell. In arc-down conditions, it is important to both protect the klystron as well as modulator from damage. Figure 6 shows measured waveforms in the cell. As shown, after the voltage across the load collapses due to an induced arc, the current rises. The rate of rise is predominately determined by the di/dt limiting inductor in the cell. As the fire switch opens to suppress the fault, the voltage across the switch rises. Using active snubbing, the voltage across the switch is kept to safe levels, not exceeding the device rating [6].

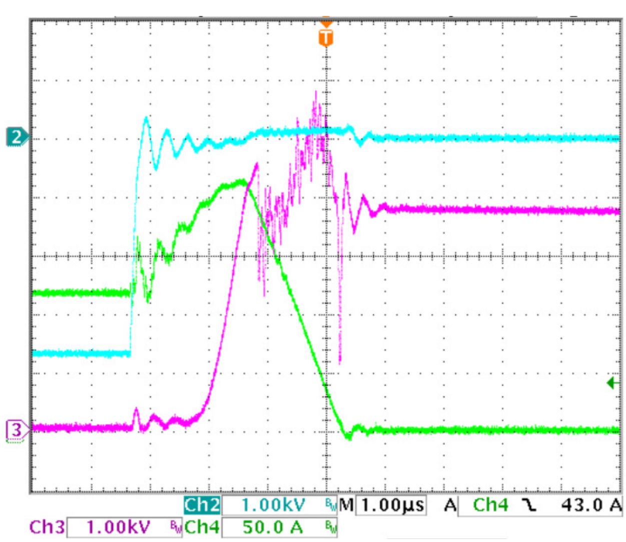

Figure 6: Experimental waveforms of cell during an induced fault. Ch. 2 (blue): load voltage, 1kV/div. Ch3 (pink): IGBT Vce, 1kV/div. Ch. 4 (green): IGBT collector current, 50 A/div.

SUMMARY AND PROJECT STATUS

This paper was a brief survey of some of the features under development for the SLAC P2 Marx. At this time, the second version of the cell is being finalized and will soon be power tested. The design for the full modulator is also nearing completion. The next major project milestone will be fabrication of the full modulator. Estimated completion is early Spring of 2011.

ACKNOWLEDGEMENT

The authors thank A. Viceral, P. Shen, D. Anderson, K. Macken, T. Tang, C. Huang, R. Esmaili, J. Olszewski, J. Hugyik, W. Gorecki, Z. Szalata, S. Zheng, C. Adolphsen, and T. Beukers for their contributions to the P2 Marx program.

REFERENCES

[1] C. Burkhart, *et al.*, “P1-Marx modulator for the ILC,” 2010 IEEE Power Modulator Conference, Atlanta, GA, 2010.

[2] K. Macken, *et al.*, “Towards a PEBB-based design approach for a Marx-topology ILC klystron modulator,” PAC’09, Vancouver, Canada, May 2009.

[3] M.A. Kemp, *et al.*, “Status update on the second-generation ILC Marx modulator prototype,” 2010 Power Modulator Conference, Atlanta, GA, 2010.

[4] K. Macken, *et al.*, “A hierarchical control architecture for a PEBB-based ILC Marx modulator,” in proc. IEEE pulsed power conf., Washington DC, June 29-July 2, 2009, pp. 826-831.

[5] A. Benwell, *et al.*, “A prognostic method for scheduling maintenance on the P2-Marx modulator,” 2010 IEEE Power Modulator Conference, Atlanta, GA, 2010.

[6] M.N. Nguyen, *et al.*, “Compact, intelligent, digitally controlled IGBT gate drivers for a PEBB-based ILC Marx modulator,” IPAC’10, Kyoto, Japan, May 2010.

[7] M.A. Kemp, *et al.*, “Lifetime tests on a high ohms/square metalized high crystalline polypropylene film capacitor,” 2010 IEEE Power Modulator Conference, Atlanta, GA, 2010.

[8] F. Wang, *personal communication.*